ELSEVIER

Nuclear Instruments and Methods in Physics Research A 469 (2001) 47–54

NUCLEAR INSTRUMENTS & METHODS IN PHYSICS RESEARCH Section A

www.elsevier.com/locate/nima

# The HERMES forward tracking chambers: construction, operation, and aging effects

J.T. Brack[a,*], J.E. Belz[a], S. Clark[a], J. Ely[a], B. Fox[a], G.J. Hofman[a], E.R. Kinney[a], D.J. Mercer[a], G. Rakness[a], R.A. Ristinen[a], W.R. Smythe[a], D. Warner[b]

[a] *Department of Physics, CB 446, University of Colorado, Boulder 80309-0446, USA*
[b] *Department of Physics, Colorado State University, Fort Collins, CO 80523, USA*

Received 6 December 2000

**Abstract**

The design, construction and operation of the HERMES forward (front) tracking chambers and associated electronics are described. Resolution and limited aging tests have been performed on these drift chambers, which use an $Ar/CF_4/CO_2$ (90 : 5 : 5) gas mixture. No degradation in chamber performance has been observed for a cumulative charge in excess of 9 C/cm. © 2001 Elsevier Science B.V. All rights reserved.

*PACS:* 29.40.Cs; 07.89.+b

*Keywords:* Wire chamber; $CF_4$ gas; Aging studies; Radiation damage; HERMES spectrometer; Resolution studies

## 1. Introduction

The HERMES experiment uses the deep-inelastic scattering (DIS) of polarized lepton beams from polarized nucleon targets primarily to study the spin structure of the nucleon [1–4]. The experiment uses a forward-angle spectrometer to detect scattered leptons and hadronic reaction products from an (fixed) internal gas target. The spectrometer is essentially comprised of a large dipole magnet instrumented with tracking chambers in front and behind as well as inside the region of the gap. Particle identification is performed using a Cherenkov detector, a transition-radiation detector, and a lead-glass calorimeter augmented with a pre-shower detector. Further details may be found in Ref. [5]. Commissioning of the spectrometer was completed in the summer of 1995, allowing spin structure measurements [1] from the polarized $^3$He target [6] in the fall of that year. The present work focuses on the set of multiwire drift chambers located just forward of the magnet aperture, the so-called front chambers (FCs), which have been operated successfully during the entire 1995–2000 period.

The FCs are drift chambers of a standard design with alternating anode–cathode wire geometry as shown in Fig. 1. Significant savings in construction costs were achieved using an economical method to produce the required wire support frames with

*Corresponding author. Tel.: +1-303-492-3660; fax: +1-303-492-7486.

*E-mail addresses:* brack@drax.colorado.edu (J.T. Brack), gertjan.hofman@colorado.edu (G.J. Hofman).

0168-9002/01/$ - see front matter © 2001 Elsevier Science B.V. All rights reserved.
PII: S0168-9002(01)00710-0

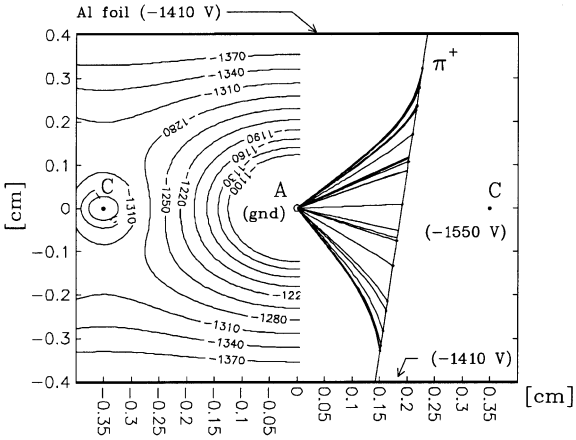


Fig. 1. Layout of a single cell showing dimensions, applied high voltages on the anodes (A) and cathode (C) and potential contours (calculated using Garfield [7]) for one half of the cell. A single cathode plane at −1410 V separates this layer from the next layers (not shown). Also shown are typical electron drift tracks generated by a 2 GeV pion.

metal traces for signal transmission and HV distribution. Also of interest is the operational experience with the particular gas mixture used in the experiment, since little was known about the long term effects of high rate operation of chambers with gas mixtures containing $CF_4$.

## 2. Mechanical design

Each chamber consists of six wire planes, with 96 anode wires per plane. The anodes are gold-plated tungsten wires of 20 μm diameter spaced every 7 mm. The wires of the middle two planes are vertical, while those of the first and last pairs of planes are tilted by +30° and −30° from the vertical, respectively. The second plane of each pair has the wire positions staggered by 3.5 mm to help resolve the left/right ambiguity. Field shaping wires made from 76 μm[1] Au-plated Al are strung between the sense wires, and 6.4 μm thick double-sided aluminized Mylar cathode foils are interleaved with the wire planes producing 'cells' that are 7 mm wide and 8 mm deep. Foils and wires are supported by fiberglass epoxy (G10) frames. A pair of thicker outer foils contains the gas volume and eliminates any pressure differential on the cathode foils. A pair of 1.27 cm thick outer Al frames provides rigidity while supporting gas, power, alignment targets, mounting hardware, and a Faraday box for the amplifier electronics. By fabricating printed circuit boards of only the minimal necessary size to contain the metal traces, a substantial reduction in cost was obtained, relative to the method of applying traces to the entire G10 support frame.

[1] The diameter value published in Ref. [5] was an error.

## 3. Construction

Each wire plane was built up from layers of machined G10 boards, shown in Fig. 2. The 68 × 22 cm opening in the first layer, or sub-frame, defines the active area. Circuit boards were glued along the upper and lower edges of this active area, providing anode wire soldering pads and output traces on the upper board, and a cathode-wire bus on the lower board. These circuit boards were precisely located on the sub-frame using dowel pins. Also glued to the sub-frame were circuit boards with traces for the HV feed to the cathode foils.

After the circuit boards were glued to the sub-frame, cathode and anode wires were installed at 50 g tension using a wire winding machine at the

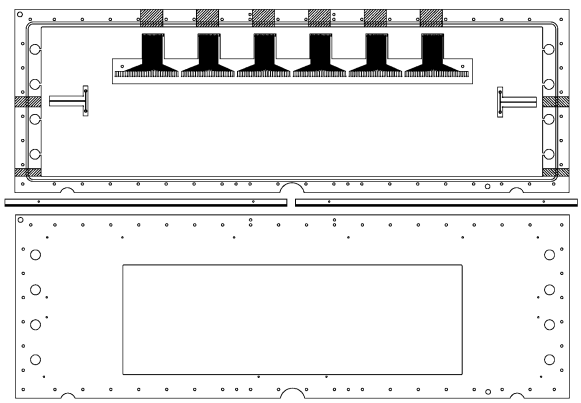

Fig. 2. The sub-frame (lower) and sealing frame (upper) G10 pieces that make up a plane. Also shown are the circuit boards, and the relieved surfaces (hatched areas) in the sealing frame where the circuit boards exit the wire chamber.

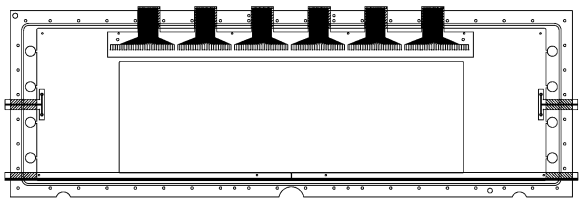

Fig. 3. The assembled plane, shown as an overlay of the pieces in the previous figure.

Los Alamos Natl. Lab. The ends of the anode and cathode wires were soldered onto their respective circuit boards. Note only one end of each wire ended in a soldered joint; the other end was secured in a strip of epoxy running the length of the board. Measured wire placement precision averaged about 4 μm ($\sigma$) in spacing and 0.02° in angle.

The final G10 'sealing frame' layer was epoxied over the circuit board layer. The thickness of the sub-frame plus the circuit board layer make up half the cell thickness. The sealing frame layer provides the remaining thickness and has an O-ring groove on its upper surface for sealing to the next plane. A layer of Mylar, aluminized on both sides, was glued to the bottom of the sub-frame, completing the plane (see Fig. 3).

## 4. Electronics

A significant constraint on electronics design is the low profile of electronic components required by the 8 mm plane spacing; no commercially available card had sufficiently low profile. The pre-amplifier/discriminator cards are a TRIUMF laboratory modification of the LeCroy 2735DC card and use LeCroy TRA402S amplifiers and LeCroy MVL407S comparators. In particular, a low noise front end and a pulse shaper were added. Channel-to-channel gain variation is reduced to about 10% using a common emitter mode input transistor (MMBR941LT1) with feedback. Input impedance is about 200 Ω. This input stage also provides a pole-zero differentiation to reduce the tail of the anode signal and hence improve the rate capability. A second filter is placed just before the comparator.

The threshold control lines require 0 to +10 V, corresponding to approximately 0.07 to 1.2 μA at the comparator input. At 0 V on the threshold it is estimated that the comparators will fire with near 100% efficiency on a charge of 12,000 electrons or more. The chosen settings (about 0.25 V) are those high enough to prevent oscillation of the cards yet also provide sufficient efficiency. Crosstalk of 3.5% between neighboring channels is typical. The 144 cards used on the four wire chambers at HERMES draw a total of 77 A at −5.6 V and 44 A at +5.3 V. Since this yields a high power density, the cards are cooled by forced air flow using blowers. Air temperature within the air channel of each chamber is typically 31°C, and is monitored using semiconductor probes.

## 5. Operation

The FC's use a gas mixture of 5% $CO_2$, 5% $CF_4$ and 90% Ar (by volume) at a pressure slightly above atmosphere. This choice of gas was largely determined by three factors. This mixture meets the DESY criteria for nonflammability, essential for operation in an underground tunnel. It has a fast electron drift velocity, allowing high rates. Lastly, gas mixtures with $CF_4$ are known to reduce aging effects [8]. A gas recycling system built at TRIUMF Laboratory recycles 80% of the gas volume. Filters in the recycling system remove $O_2$ and $H_2O$ contamination.

The high-voltage operating values are −1410 V on the cathode foils and −1550 V on the field shaping wires. Sense wires and outermost foils are kept at ground.

## 6. Chamber performance

The performance of the HERMES FC's was initially studied using DIS scattering data obtained at the HERMES experiment. The single plane efficiency is excellent, rising from 97% near the anode wire to 99% at the center and edge of the cell [5]. The chamber spatial resolution, shown in Fig. 4, was determined by using hit information of all the FC planes except for the one under study.

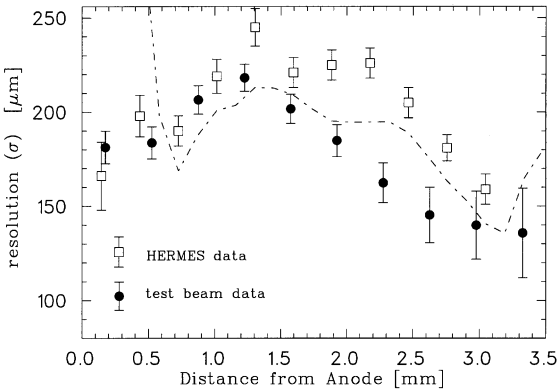


Fig. 4. FC resolution as determined from HERMES scattering data using hadrons (open squares) as well as from the electron beam test study (solid circles). For the latter data the errors are dominated by systematics due to the determination of the beam position by the surrounding chambers. The dashed line is a GARFIELD model calculation scaled up by a factor of 2.

To extract the resolution, the residual ($= x_{\mathrm{trk}} - x_{\mathrm{fc}}$, the difference between calculated position of the track and that determined using a plane) width observed in the planes used in the track fit is first measured. This distribution width is assumed to be constant and independent of the plane or location of track relative to the anode wire. It is then subtracted quadratically from the residual width observed in the plane under study.

The resulting resolution versus track position data (Fig. 4, open squares) is not completely understood. In particular, the resolution of these chambers is poorest in the center of the drift cell instead of at the edges of the cell as is observed in other drift chambers. It was decided to study the performance of one of the spare front chambers in an electron test beam at DESY.

For this measurement a spare front chamber was surrounded by three small chambers. These calibration chambers consist of a regular anode–cathode configuration with 6 mm wide cathode pick-up strips parallel and perpendicular to the anode wires. The induced pulses on the strips travel down a delay line and are discriminated by a constant fraction type discriminator. The observed resolution for strips perpendicular to the anode wires was approximately 230 μm ($\sigma$) resulting in a beam definition at the FC planes under study of $130 \pm 7$ μm.

A new standard drift-time relationship (SDTR) was calculated for the front chamber using the track definition from the delay-line chambers only. Differences between this SDTR and the one previously determined using tracking in HERMES were small, except near the edges of the cell. The extracted chamber resolution is shown in Fig. 4 and compared to the resolution extracted from HERMES DIS data.

The two curves show similar behavior—the resolution is worst at the cell center and improves near the cathode wire. Some differences in the two results can be expected due to the different analyses. One possible explanation is that, due to the weak electric field near the edges of the cell, only electrons generated near the track center can reach the anode wires, reducing arrival time jitter. However, a reduced efficiency near the edge of the cell might be expected but not observed. Anode pulse heights (not measured in this test) should also be reduced.

Also shown in this figure is the spatial resolution predicted by the GARFIELD program [7]. This simulation used $Ar/CF_4/CO_2$ drift velocities as determined by the HERMES group [6] for calibrating the spectrometer's back chambers. A fixed gas gain of $2 \times 10^4$ was applied—other gas gain models were also used but without significant change in the result. The pulse arrival time (triggering threshold) was determined to be the point at which the output current exceeded 100 nA. Electronic response to the generated signal was not simulated. While the shape of the chamber resolution curve is reasonably well reproduced, the magnitude is underestimated.

In order to understand the influence of the $CO_2$ component, the gas mixture was changed from the standard ratio 90 : 5 : 5 $Ar/CF_4/CO_2$ to 87 : 5 : 8 and 93 : 5 : 2. Although the drift velocity decreased (increased) for the the 87 : 5 : 8 (93 : 5 : 2) mixture, no significant change in resolution was observed.

## 7. Aging studies

In the absence of pre-existing data on the aging of wire chambers using the standard HERMES gas mixture of 90 : 5 : 5 $Ar/CO_2/CF_4$, the

HERMES tracking group has been concerned about possible damage to the HERMES chambers over extended running times. Radiation damage with prolonged exposure is common for chambers running with many gas mixtures, and usually is first detectable as a decrease in gain and increased dark current. The effect is caused by deposits on the conducting surfaces of the chambers, resulting from the chemistry of the ionized gas.

Studies have been conducted at TRIUMF [8,9], using a variety of gas mixtures, revealing the effects of exposure rates and gas flow rates. Most interesting in these experiments was the apparent immunity to damage, under most conditions, of chambers using $CF_4$ in the gas mix. Although not completely understood, this immunity has been ascribed to the reactive characteristics of fluorine, scavenging impurities and carrying them from the chamber in the normal gas flow. While it was hoped that addition of $CF_4$ to the gas mix would give this rejuvenating effect to the HERMES chambers, there has been no proof until now.

### 7.1. Method

While a complete test of the 90 : 5 : 5 mix would involve repeated measurements with varying gas flow rates, irradiation rates and HV settings, the intent here was to demonstrate chamber longevity in as short a time as possible, so a single measurement was made under extreme conditions.

A single-plane chamber was made by removing five planes from the prototype HERMES front chamber. Gas of the standard HERMES mix, 90 : 5 : 5 $Ar/CO_2/CF_4$, flowed from a pre-mixed bottle through the chamber at a rate of six volume changes per day. The chamber was operated with $-1510$ V on the cathodes (wires and foils) creating a gas gain of about $5 \times 10^5$. For comparison, the HERMES gas recycling system circulates about 40 volume changes per day through the FCs, and the gas gain is approximately $2 \times 10^4$.

Cosmic rays were used to monitor the gain. Near-vertical trajectories were defined by two 5 cm diameter scintillators placed immediately above and below the chamber. The scintillators were centered on one of the six groups of 16 anodes. Only the signals from this anode group were examined; the other 80 anodes were not grounded and drew no current. The 16 anodes were bussed together at the chamber pin connector, and a 2 MΩ resistor to ground kept the anodes at zero voltage. A single signal wire went to an amplifier[2], and then to a CAMAC ADC (LeCroy 2249A). Look At Me (LAM) signals were generated by scintillator coincidences, and the CAMAC crate was read by a PC and written to disk on each LAM. Also recorded with each event was the atmospheric pressure, measured with a current producing pressure transducer, which was read from a separately gated ADC. The pressure transducer was calibrated against the NCAR [10] weather station, in Boulder.

A 1 mCi $^{90}Sr$ β-emitting source was used to irradiate the chamber. The procedure was to remove the upper scintillator, center the source in its place, 24 mm above the anode wires, and leave it for a week. Then the source was removed, the scintillator replaced, and the anode gain was measured overnight using cosmic rays.

With the source in place, the singles rate on the lower scintillator was about 1 MHz. The circular illuminated anode region was about 700 $mm^2$, covering sections of four anodes. Because of the 7 mm anode pitch, one linear cm of cell contains 70 $mm^2$, so that a total of approximately 10 cm of anode wire was illuminated by the source, giving an average rate of $10^5$/cm s.

Two comparisons can be made to the average test chamber rate of $10^5$ particles/cm s with the source in place. First, this is about 40 times the average HERMES FC rate (50 kHz on a 20 cm wire for normal polarized target running), so that 1 week with the source simulates roughly a HERMES year. Second, for comparison with previous aging tests, the current draw at this rate is about 10 μA on 10 cm of wire, or about 0.5 C/cm in a 6-day run. The experiment was run for 17 weeks, for a cumulative effect of about 9 C/cm on the anodes, which is comparable to the longest previous tests of other gas mixtures containing $CF_4$ [8,9].

[2] LAMPF Electronics Equipment Pool wire chamber amplifier/discriminator, uses LeCroy MVL100 preamp/disc chips, gain × 10.

### 7.2. Results

Fig. 5 shows the mean gain as a function of average absolute atmospheric pressure for each of the data runs over the duration of the experiment. A line was fit to the data, and used to correct the gain for each run to an average normal absolute atmospheric pressure of 850 mbar at Boulder's altitude of 1600 m. The pressure varied during each run, sometimes by 20 mbar or more. The effects of these variations were examined by gating the data for each run into 2 mbar bins and refitting the straight line. A small change in the slope was observed (0.1 bins/mbar), but it made no difference in the conclusions.

The pressure-compensated data are shown in Fig. 6 as a function of accumulated charge. The bulk of the data indicate a trend of slowly increasing gain with accumulated charge. The first two runs, and the last run using new anode wires, are shown (open points) near zero accumulated charge, and were omitted from the linear least squares fit. It is unclear why runs 1 and 2 give abnormally high gain. It is doubtful that such severe degradation of gain could occur in the first 0.25 C accumulated charge. It is more likely that a shift occurred somewhere in the electronics, which appear stable throughout the rest of the experiment. The final measurement (circle) on a previously unused section of the chamber probably gives a more likely measurement of gain at zero accumulated charge. If this point is included in the least squares fit, the slope is still positive (0.4%/C). It should be noted that Openshaw et al. [8] also measured a slight positive increase in gain with exposure for a gas mixture containing small amounts of $CF_4$ (48 : 48 : 4 Ar/Eth/$CF_4$).

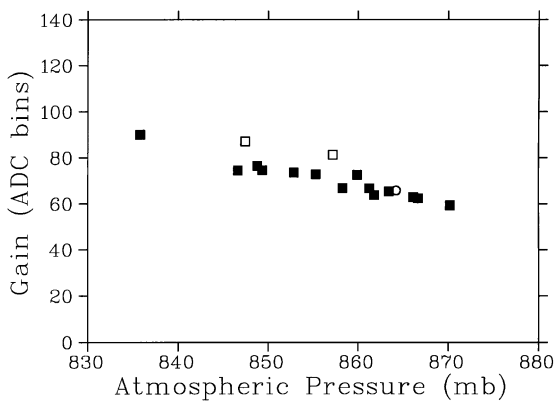


Fig. 5. Mean gain as a function of atmospheric pressure (solid squares). The gain versus pressure relationship was generated from the full data set minus the first two runs, which are included in the figure (open squares). Also included is the data point taken at the end of the test on a fresh set of anodes (open circle).

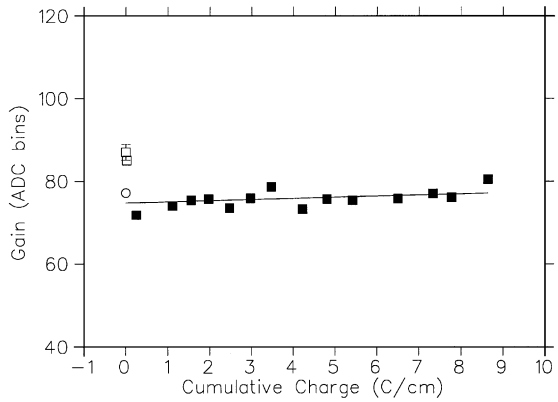


Fig. 6. Pressure corrected mean gain as a function of accumulated charge on the anode wires. Symbols as in Fig. 1.

The stability of gain after long exposures exists in spite of foil etching. When the chamber was opened at the end of the test, the exact location of the source was immediately obvious from circular etched regions on the upper and lower foils (see Fig. 7). The etching is most severe nearest to the exposed sections of anodes, and is minimal near the cathodes. The resistance across the etched sections of foils near the anodes is large (> 1 MΩ/cm) compared to the usual resistance (< 10 Ω/cm) on the aluminized foil, indicating that the majority of the aluminum has been removed. Still, neither the gain nor the efficiency of the chamber were measurably affected.

One anode wire and one cathode wire were removed from the exposed region of the chamber. Two 1 cm sections were clipped from each wire, one from within the exposed region and one from the un-exposed end of the wire. The four samples were examined under a scanning electron microscope. No difference was observed between the exposed and un-exposed sections of the anode

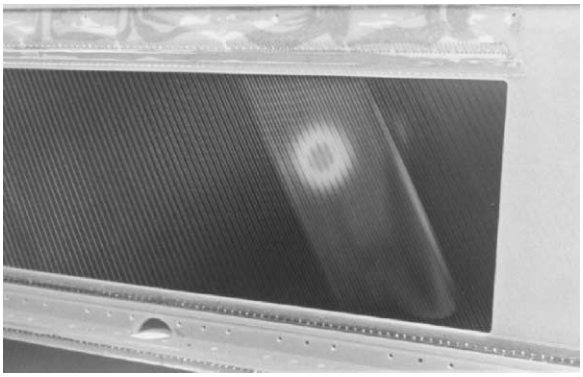

Fig. 7. A picture of the plane, showing etching of the cathode foil.

wire; both sections appeared without deposits as shown in Fig. 8. While the un-exposed cathode section also appeared undamaged in any way, the exposed cathode section had deposits of 20 to 30 μm in diameter, occurring approximately 1 per mm of wire length, as shown in Fig. 9. X-ray fluorescence spectra of the deposits and an undamaged region of the same cathode sample were compared, showing the deposits contain chlorine. The elements Au, Al, Cu, and Ni, identified in both spectra, came from the wire production process, which begins with Cu clad Al wire which then receives a thin 'strike' of Ni before

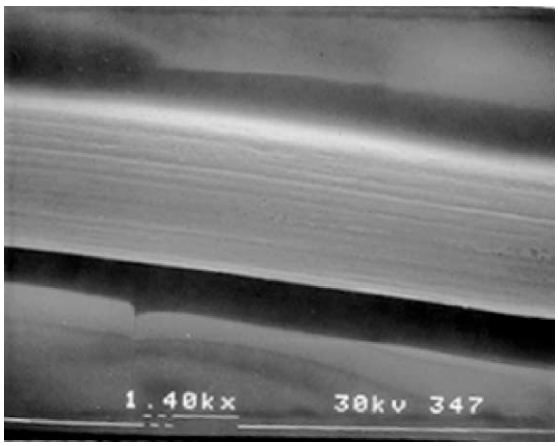


Fig. 8. A picture of a section of the exposed 20 μm anode wire, taken with a scanning electron microscope at magnification of 1400×.

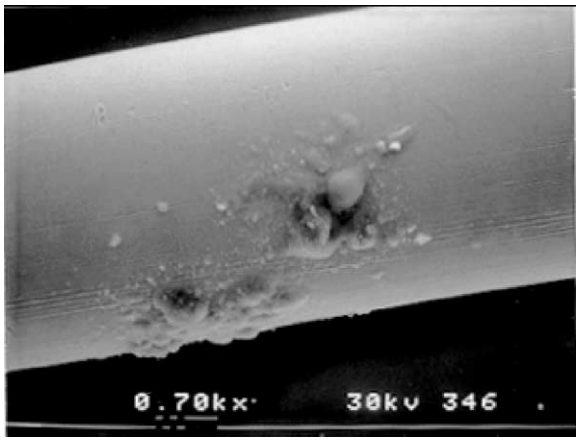


Fig. 9. A picture of a section of the exposed 50 μm cathode wire, as in Fig. 8 but with magnification of 700×, showing the deposits created during the irradiation.

being coated with Au. Oxygen was also observed in both samples.

### 7.3. Conclusions

This aging test was a crude, single-purpose test, to investigate the aging behavior of a wire chamber using the 90 : 5 : 5 $Ar/CO_2/CF_4$ gas mixture. As such, there was a lack of systematic studies that would allow us to draw strong conclusions.

Furthermore, there are features of the test that may restrict the validity of the results. First, it has been pointed out [11] that the intense sources used in aging tests lead to space-charge effects that limit electron drift velocities near the anode wire. This may change the chemistry of the aging process which we have attempted to measure. For example, Openshaw et al. [8] measured gain reduction of a factor of 2 at current density of 0.25 μA/cm for the cells used in their test, at nominal gas gain of $5 \times 10^4$. In the Boulder test, the gain with the high rate $^{90}Sr$ source in place was measured to be reduced by 20% from that at cosmic ray rates, at much higher nominal gas gain (about $5 \times 10^5$) and higher current density (1 μA/cm).

Second, operating chambers at 1650 m altitude may affect the aging process because of the reduction in gas density. This expands the distance

between collisions for the drifting electrons, allowing higher maximum drift velocities. This may partially compensate for the reduction in drift velocity due to space charge generation described above, but the degree to which this occurs has not been measured in this test.

With the above caveats, the conclusion of this test is that we have been absolutely unable to degrade the chamber performance after a cumulative exposure of some 9 C/cm on the wires. In spite of foil etching and the deposits on the cathode wires, chamber efficiency at the end of the test was indistinguishable from what it was at the beginning.

## Acknowledgements

We gratefully acknowledge the assistance of Val Armijo and Lee Atencio with the construction of the chambers at the Los Alamos National Laboratory. We also acknowledge the extensive advice and discussions with C.A. Miller (TRIUMF) on all aspects of the chamber design. Others from TRIUMF whom we would like to acknowledge are Peter Bennett (TRIUMF) for assistance in the design and fabrication of the electronics for the onboard amplification, shaping and discrimination of the wire signals, and Robert Openshaw and Martin Kueckes for their design and construction of the gas system for the front chambers. Finally, we are grateful to Yorck Holler (DESY) for his patience and ceaseless help in providing the resources and infrastructure for the installation of the chambers.

## References

[1] K. Ackerstaff et al., Phys. Lett. B 404 (1997) 383.
[2] A. Airapetian et al., Phys. Lett. B 442 (1998) 484.
[3] K. Ackerstaff et al., Phys. Lett. B 464 (1999) 123.
[4] A. Airapetian et al., Phys. Rev. Lett. 84 (2000) 2584.
[5] K. Ackerstaff et al. [HERMES Collaboration], Nucl. Instr. and Meth. A 417 (1998) 230.
[6] S. Bernreuther et al., Nucl. Instr. and Meth. A 416 (1998) 45, hep-ex/9803005.
[7] R. Veenhof, Garfield: a drift chamber simulation program v.512, CERN program library entry W5050, 1991.
[8] R. Openshaw, R. Henderson, W. Faszer, D. Murphy, M. Salomon, G. Sheffer, IEEE Trans. Nucl. Sci. NS-36 (1989) 567.
[9] R. Henderson, R. Openshaw, W. Faszer, M. Salomon, G. Salomons, G. Sheffer, IEEE Trans. Nucl. Sci. NS-35 (1988) 477.
[10] National Center for Atmospheric Research, Boulder CO, see http://www.atd.ucar.edu/cgi-bin/mlabweather.
[11] J. Vavra, Nucl. Instr. and Meth. A 252 (1986) 547.